Buckling of Long Sandwich Cylindrical Shells Under External Pressure

G. A. Kardomateas
Professor of Aerospace Engineering
Fellow ASME
e-mail: george.kardomateas@aerospace.gatech.edu

G. J. Simitses[1]
Professor Emeritus of Aerospace Engineering
Fellow ASME

Georgia Institute of Technology,
Atlanta, GA 30332-0150

An elasticity solution to the problem of buckling of sandwich long cylindrical shells subjected to external pressure is presented. In this context, the structure is considered a three-dimensional body. All constituent phases of the sandwich structure, i.e., the facings and the core, are assumed to be orthotropic. The loading is a uniform hydrostatic pressure, which means that the loading remains normal to the deflected surface during the buckling process. Results are produced for laminated facings, namely, boron/epoxy, graphite/epoxy and kevlar/epoxy laminates with 0 deg *orientation with respect to the hoop direction, and for alloy-foam core. Shell theory results are generated with and without accounting for the transverse shear effect. Two transverse shear correction approaches are compared, one based only on the core, and the other based on an effective shear modulus that includes the face sheets. The results show that the shell theory predictions without transverse shear can produce highly non-conservative results on the critical pressure, but the shell theory formulas with transverse shear correction produce reasonable results with the shear correction based on the core only being in general conservative (i.e., critical load below the elasticity value). The results are presented for four mean radius over shell thickness ratios, namely 15, 30, 60, and 120 in order to assess the effect of shell thickness (and hence that of transverse shear). For the same thickness, the differences between elasticity and shell theory predictions become larger as the mean radius over thickness ratio is decreased. A comparison is also provided for the same shell with homogeneous composite construction. It is shown that the sandwich construction shows much larger differences between elasticity and shell theory predictions than the homogeneous composite construction. The solution presented herein provides a means of a benchmark for accurately assessing the limitations of shell theories in predicting stability loss in sandwich shells.* [DOI: 10.1115/1.1934513]

Introduction

The need for lightweight, yet stiff and durable structures has made the sandwich composite configuration a leading edge technology with promise for innovative high performance structural designs. A typical sandwich structure is composed of two thin metallic or composite laminated faces and a thick soft core made of foam or low strength honeycomb. This lightweight sandwich construction is of great interest in the design and manufacture of aircraft, spacecraft, and marine vehicles. In addition to the high specific stiffness and strength, sandwich construction offers enhanced corrosion resistance, noise suppression, and reduction in life-cycle costs.

There are several issues and questions related to the use of sandwich construction that require attention and answers. In applications involving compressive loading, loss of stability and the accurate prediction of buckling loads is of major concern. This is particularly important in sandwich construction because of the existence of the low-modulus core, which would be expected to make transverse shear effects even more significant than in homogeneous composites. In addition, composite sandwich structures are normally envisioned in applications involving relatively thick construction, therefore thickness effects need to be properly accounted for.

Shell theory solutions for buckling and even initial postbuckling behavior have been produced by many authors (e.g., from the 60's, Hutchinson [1]; Budiansky and Amazigo [2], many of these works with elegant variational formulations). Indeed, the existence of different shell theories underscores the need for benchmark elasticity solutions, in order to compare the accuracy of the predictions from the classical and the improved shell theories. Several elasticity solutions for monolithic homogeneous composite shell buckling have become available. In particular, Kardomateas [3] formulated and solved the problem for the case of uniform external pressure and orthotropic homogeneous material; in this study, just as in the present one, a long shell was studied ("ring" assumption). This simplifies the problem considerably, in that the pre-buckling stress and displacement field is axisymmetric, and the buckling modes are two dimensional, i.e., no axial component of the displacement field, and no axial dependence of the radial and hoop displacement components. The ring assumption was relaxed in a further study [4], in which a nonzero axial displacement and a full dependence of the buckling modes on the three coordinates was assumed. Other three-dimensional elasticity buckling studies are the buckling of a transversely isotropic homogeneous thick cylindrical shell under axial compression [5] and a generally cylindrically orthotropic homogeneous shell under axial compression [6]. In addition, three-dimensional elasticity results, again for homogeneous hollow cylinders subjected to combined axial compression and uniform external pressure, were provided by Soldatos and Ye [7] based on a successive approximation method.

The geometry of a circular cylindrical shell is particularly at-

[1]Also, Professor Emeritus of Aerospace Engineering, University of Cincinnati, Cincinnati, OH 45221-0070.

Contributed by the Applied Mechanics Division of THE AMERICAN SOCIETY OF MECHANICAL ENGINEERS for publication in the ASME JOURNAL OF APPLIED MECHANICS. Manuscript received by the Applied Mechanics Division, June 5, 2002; final revision, July 9, 2004. Associate Editor: N. Triantafyllidis. Discussion on the paper should be addressed to the Editor, Prof. Robert M. McMeeking, Journal of Applied Mechanics, Department of Mechanical and Environmental Engineering, University of California-Santa Barbara, Santa Barbara, CA 93106-5070, and will be accepted until four months after final publication in the paper itself in the ASME JOURNAL OF APPLIED MECHANICS.

tractive for constructing elasticity solutions due to the axisymmetry which simplifies the analysis. Furthermore, a prerequisite to obtaining elasticity solutions for shell buckling such as the one by Kardomateas [3], is the existence of three-dimensional elasticity solutions to the pre-buckling problem. Elasticity solutions for monolithic homogeneous orthotropic cylindrical shells have been provided by Lekhnitskii [8]. Recently, elasticity solutions for sandwich shells were obtained by properly extending the solutions for monolithic structures [9]. The latter is the pre-buckling solution needed to formulate the bifurcation problem in the elasticity context.

As far as shell theory, there are but few studies reported in the literature that deal with sandwich shell analyses [10–12]. The comparison to shell theory predictions will be based on the formulas presented in Smith and Simitses [13] and Simitses and Aswani [14] and specialized to an infinite length cylinder, whose behavior is similar to that of a sandwich ring.

Formulation

By considering the equations of equilibrium in terms of the second Piola-Kirchhoff stress tensor, subtracting these at the perturbed and initial conditions, and making order of magnitude assumptions on the products of stresses and strains/rotations, based on the fact that a characteristic feature of stability problems is the shift from positions with small rotations to positions with rotations substantially exceeding the strains, Kardomateas [3] obtained the following buckling equations:

$$\frac{\partial}{\partial r}(\sigma_{rr}-\tau^0_{r\theta}\omega_z+\tau^0_{rz}\omega_\theta)+\frac{1}{r}\frac{\partial}{\partial\theta}(\tau_{r\theta}-\sigma^0_{\theta\theta}\omega_z+\tau^0_{\theta z}\omega_\theta)+\frac{\partial}{\partial z}(\tau_{rz}-\tau^0_{\theta z}\omega_z+\sigma^0_{zz}\omega_\theta)+\frac{1}{r}(\sigma_{rr}-\sigma_{\theta\theta}+\tau^0_{rz}\omega_\theta+\tau^0_{\theta z}\omega_r-2\tau^0_{r\theta}\omega_z)=0, \quad (1a)$$

$$\frac{\partial}{\partial r}(\tau_{r\theta}+\sigma^0_{rr}\omega_z-\tau^0_{rz}\omega_r)+\frac{1}{r}\frac{\partial}{\partial\theta}(\sigma_{\theta\theta}+\tau^0_{r\theta}\omega_z-\tau^0_{\theta z}\omega_r)+\frac{\partial}{\partial z}(\tau_{\theta z}+\tau^0_{rz}\omega_z-\sigma^0_{zz}\omega_r)+\frac{1}{r}(2\tau_{r\theta}+\sigma^0_{rr}\omega_z-\sigma^0_{\theta\theta}\omega_z+\tau^0_{\theta z}\omega_\theta-\tau^0_{rz}\omega_r)=0, \quad (1b)$$

$$\frac{\partial}{\partial r}(\tau_{rz}-\sigma^0_{rr}\omega_\theta+\tau^0_{r\theta}\omega_r)+\frac{1}{r}\frac{\partial}{\partial\theta}(\tau_{\theta z}-\tau^0_{r\theta}\omega_\theta+\sigma^0_{\theta\theta}\omega_r)+\frac{\partial}{\partial z}(\sigma_{zz}-\tau^0_{rz}\omega_\theta+\tau^0_{\theta z}\omega_r)+\frac{1}{r}(\tau_{rz}-\sigma^0_{rr}\omega_\theta+\tau^0_{r\theta}\omega_r)=0. \quad (1c)$$

In the previous equations, σ^0_{ij} and ω^0_j are the values of stresses and rotations, respectively, at the initial equilibrium position (pre-buckling state), and σ_{ij} and ω_j are the corresponding values at the perturbed position (buckled state).

The boundary conditions associated with Eq. (1) were obtained from the traction (stress resultant) relationships in terms of the second Piola-Kirchhoff stress tensor, and by further considering the fact that because of the hydrostatic pressure loading, the magnitude of the surface load remains invariant under deformation, but its direction changes (since hydrostatic pressure is always directed along the normal to the surface on which it acts). By writing these equations for the initial and the perturbed equilibrium position and then subtracting them and using the previous arguments on the relative magnitudes of the rotations, Kardomateas [3] obtained the following boundary conditions on a surface which has outward unit normal $(\hat{\ell},\hat{m},\hat{n})$:

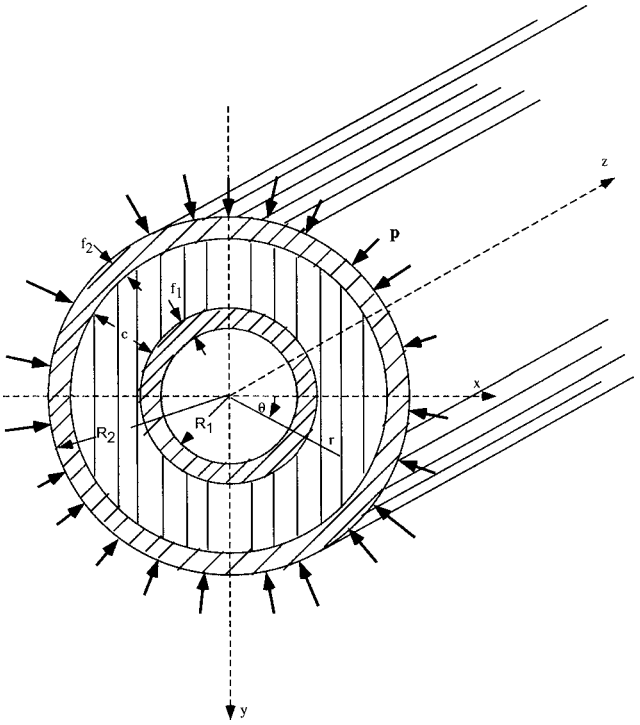

Fig. 1 Definition of the geometry and the loading

$$(\sigma_{rr}-\tau^0_{r\theta}\omega_z+\tau^0_{rz}\omega_\theta)\hat{\ell}+(\tau_{r\theta}-\sigma^0_{\theta\theta}\omega_z+\tau^0_{\theta z}\omega_\theta)\hat{m}+(\tau_{rz}-\tau^0_{\theta z}\omega_z+\sigma^0_{zz}\omega_\theta)\hat{n}=p(\omega_z\hat{m}-\omega_\theta\hat{n}), \quad (2a)$$

$$(\tau_{r\theta}+\sigma^0_{rr}\omega_z-\tau^0_{rz}\omega_r)\hat{\ell}+(\sigma_{\theta\theta}+\tau^0_{r\theta}\omega_z-\tau^0_{\theta z}\omega_r)\hat{m}+(\tau_{\theta z}+\tau^0_{rz}\omega_z-\sigma^0_{zz}\omega_r)\hat{n}=-p(\omega_z\hat{\ell}-\omega_r\hat{n}), \quad (2b)$$

$$(\tau_{rz}+\tau^0_{r\theta}\omega_r-\sigma^0_{rr}\omega_\theta)\hat{\ell}+(\tau_{\theta z}+\sigma^0_{\theta\theta}\omega_r-\tau^0_{r\theta}\omega_\theta)\hat{m}+(\sigma_{zz}+\tau^0_{\theta z}\omega_r-\tau^0_{rz}\omega_\theta)\hat{n}=p(\omega_\theta\hat{\ell}-\omega_r\hat{m}). \quad (2c)$$

For the lateral bounding surfaces, $\hat{m}=\hat{n}=0$ and $\hat{\ell}=1$. These conditions will also be used when we impose traction continuity at the core/face sheet interfaces.

Pre-buckling State. The problem under consideration is that of a sandwich hollow cylinder deformed by uniformly distributed external pressure, p (Fig. 1) and of infinite length (generalized plane deformation assumption). Then, not only the stresses, but also the displacements do not depend on the axial coordinate. Alternatively, this is the assumption we would make if the cylinder were securely fixed at the ends. An elasticity solution to this problem was provided by Kardomateas [9]. The solution is an extension of the classical one by Lekhnitskii [8] for a homogeneous, orthotropic shell and was provided in closed form. All three phases, i.e., the two face sheets and the core were assumed to be orthotropic. Moreover, there were no restrictions as far as the individual thicknesses of the face sheets and the sandwich construction could be asymmetric.

In this configuration, the axially symmetric distribution of external forces produces stresses identical at all cross sections and dependent only on the radial coordinate r. We take the axis of the body as the z axis of the cylindrical coordinate system and we denote by R_1 and R_2 the inner and outer radii. Let us also denote

each phase by i where $i=f_2$ for the outer face sheet, $i=c$ for the core, and $i=f_1$ for the inner face sheet. Then, for each phase, the orthotropic strain-stress relations are

$$\begin{bmatrix} \epsilon_{rr}^{(i)} \\ \epsilon_{\theta\theta}^{(i)} \\ \epsilon_{zz}^{(i)} \\ \gamma_{\theta z}^{(i)} \\ \gamma_{rz}^{(i)} \\ \gamma_{r\theta}^{(i)} \end{bmatrix} = \begin{bmatrix} a_{11}^i & a_{12}^i & a_{13}^i & 0 & 0 & 0 \\ a_{12}^i & a_{22}^i & a_{23}^i & 0 & 0 & 0 \\ a_{13}^i & a_{23}^i & a_{33}^i & 0 & 0 & 0 \\ 0 & 0 & 0 & a_{44}^i & 0 & 0 \\ 0 & 0 & 0 & 0 & a_{55}^i & 0 \\ 0 & 0 & 0 & 0 & 0 & a_{66}^i \end{bmatrix} \begin{bmatrix} \sigma_{rr}^{(i)} \\ \sigma_{\theta\theta}^{(i)} \\ \sigma_{zz}^{(i)} \\ \tau_{\theta z}^{(i)} \\ \tau_{rz}^{(i)} \\ \tau_{r\theta}^{(i)} \end{bmatrix}, \quad (i=f_1,c,f_2) \tag{3}$$

where a_{ij}^i are the compliance constants (we have used the notation $1\equiv r$, $2\equiv\theta$, $3\equiv z$).

Let us introduce the following notation for constants which enter into the stress formulas and depend on the elastic properties:

$$\beta_{11}^i = a_{11}^i - \frac{a_{13}^{i\,2}}{a_{33}^i}; \quad \beta_{22}^i = a_{22}^i - \frac{a_{23}^{i\,2}}{a_{33}^i} \quad (i=f_1,c,f_2), \tag{4a}$$

$$\beta_{12}^i = a_{12}^i - \frac{a_{13}^i a_{23}^i}{a_{33}^i} \quad (i=f_1,c,f_2); \quad k_i = \sqrt{\frac{\beta_{11}^i}{\beta_{22}^i}}; \quad (i=f_1,c,f_2). \tag{4b}$$

Then, the pre-buckling stresses in each of the phases, i.e., for $i=f_1$, c, f_2, are

$$\sigma_{rr}^{0(i)}(r) = p(C_1^{(i)} r^{k_i-1} + C_2^{(i)} r^{-k_i-1}), \tag{5a}$$

$$\sigma_{\theta\theta}^{0(i)}(r) = p(C_1^{(i)} k_i r^{k_i-1} - C_2^{(i)} k_i r^{-k_i-1}), \tag{5b}$$

$$\tau_{\theta z}^{0(i)}(r) = \tau_{rz}^{(i)}(r) = \tau_{r\theta}^{0(i)}(r) = 0, \tag{5c}$$

$$\sigma_{zz}^{0(i)}(r) = p\left\{ - C_1^{(i)} \frac{(a_{13}^i + a_{23}^i k_i)}{a_{33}^i} r^{k_i-1} - C_2^{(i)} \frac{(a_{13}^i - a_{23}^i k_i)}{a_{33}^i} r^{-k_i-1} \right\}. \tag{5d}$$

Furthermore, the pre-buckling radial displacement is found to be

$$u^{0(i)}(r) = p\left[C_1^{(i)} \frac{(\beta_{11}^i + k_i \beta_{12}^i)}{k_i} r^{k_i} - C_2^{(i)} \frac{(\beta_{11}^i - k_i \beta_{12}^i)}{k_i} r^{-k_i} \right], \tag{5e}$$

the other displacements being zero, i.e., $v^{0(i)}(r)=w^{0(i)}(r)=0$.

The constants $C_1^{(i)}$, $C_2^{(i)}$ are found from the conditions on the cylindrical lateral surfaces (traction free) and the conditions at the interfaces between the phases of the sandwich structure. Specifically, the traction conditions at the face-sheet/core interfaces give two equations [9]

$$C_1^{(f_1)}(R_1+f_1)^{k_{f1}-1} + C_2^{(f_1)}(R_1+f_1)^{-k_{f1}-1} = C_1^{(c)}(R_1+f_1)^{k_c-1} + C_2^{(c)}(R_1+f_1)^{-k_c-1} \tag{6a}$$

and

$$C_1^{(c)}(R_2-f_2)^{k_c-1} + C_2^{(c)}(R_2-f_2)^{-k_c-1} = C_1^{(f_2)}(R_2-f_2)^{k_{f2}-1} + C_2^{(f_2)}(R_2-f_2)^{-k_{f2}-1}. \tag{6b}$$

The displacement continuity at the face-sheet/core interfaces gives another two equations

$$C_1^{(f_1)} \frac{(\beta_{11}^{f_1} + k_{f1}\beta_{12}^{f_1})}{k_{f1}} (R_1+f_1)^{k_{f1}} - C_2^{(f_1)} \frac{(\beta_{11}^{f_1} - k_{f1}\beta_{12}^{f_1})}{k_{f1}} (R_1+f_1)^{-k_{f1}} = C_1^{(c)} \frac{(\beta_{11}^c + k_c\beta_{12}^c)}{k_c} (R_1+f_1)^{k_c} - C_2^{(c)} \frac{(\beta_{11}^c - k_c\beta_{12}^c)}{k_c} (R_1+f_1)^{-k_c} \tag{7a}$$

and

$$C_1^{(c)} \frac{(\beta_{11}^c + k_c\beta_{12}^c)}{k_c} (R_2-f_2)^{k_c} - C_2^{(c)} \frac{(\beta_{11}^c - k_c\beta_{12}^c)}{k_c} (R_2-f_2)^{-k_c} = C_1^{(f_2)} \frac{(\beta_{11}^{f_2} + k_{f2}\beta_{12}^{f_2})}{k_{f2}} (R_2-f_2)^{k_{f2}} - C_2^{(f_2)} \frac{(\beta_{11}^{f_2} - k_{f2}\beta_{12}^{f_2})}{k_{f2}} (R_2-f_2)^{-k_{f2}}. \tag{7b}$$

Finally, the conditions of tractions at the lateral surfaces (traction-free inner surface and pressure, p, at the outer) give

$$C_1^{(f_1)} R_1^{k_{f1}-1} + C_2^{(f_1)} R_1^{-k_{f1}-1} = 0, \tag{8a}$$

$$C_1^{(f_2)} R_2^{k_{f2}-1} + C_2^{(f_2)} R_2^{-k_{f2}-1} = -1. \tag{8b}$$

The six linear Eqs. (6)–(8) can be solved for the six constants $C_1^{(i)}$, $C_2^{(i)}$, $(i=f_1,c,f_2)$. Other details of the solution can be found in Ref. [9].

Perturbed State. In the perturbed position we seek plane equilibrium modes as follows:

$$u_i(r,\theta) = U_i(r)\cos n\theta; \quad v_i(r,\theta) = V_i(r)\sin n\theta; \quad w_i(r,\theta) = 0, \quad i=f_1,c,f_2. \tag{9}$$

Substituting these in the strain versus displacement

$$\epsilon_{rr}^{(i)} = \frac{\partial u_i}{\partial r}, \quad \epsilon_{\theta\theta}^{(i)} = \frac{1}{r}\frac{\partial v_i}{\partial \theta} + \frac{u_i}{r}, \quad \epsilon_{zz}^{(i)} = \frac{\partial w_i}{\partial z}, \tag{10a}$$

$$\gamma_{r\theta}^{(i)} = \frac{1}{r}\frac{\partial u_i}{\partial \theta} + \frac{\partial v_i}{\partial r} - \frac{v_i}{r}, \quad \gamma_{rz}^{(i)} = \frac{\partial u_i}{\partial z} + \frac{\partial w_i}{\partial r}, \quad \gamma_{\theta z}^{(i)} = \frac{\partial v_i}{\partial z} + \frac{1}{r}\frac{\partial w_i}{\partial \theta} \tag{10b}$$

and rotation versus displacement relations

$$2\omega_r^{(i)} = \frac{1}{r}\frac{\partial w_i}{\partial \theta} - \frac{\partial v_i}{\partial z}, \quad 2\omega_\theta^{(i)} = \frac{\partial u_i}{\partial z} - \frac{\partial w_i}{\partial r}, \quad 2\omega_z^{(i)} = \frac{\partial v_i}{\partial r} + \frac{v_i}{r} - \frac{1}{r}\frac{\partial u_i}{\partial \theta} \tag{10c}$$

and then using the stress-strain relations in terms of the stiffness constants, c_{ij}^i

$$\begin{bmatrix} \sigma_{rr}^{(i)} \\ \sigma_{\theta\theta}^{(i)} \\ \sigma_{zz}^{(i)} \\ \tau_{\theta z}^{(i)} \\ \tau_{rz}^{(i)} \\ \tau_{r\theta}^{(i)} \end{bmatrix} = \begin{bmatrix} c_{11}^i & c_{12}^i & c_{13}^i & 0 & 0 & 0 \\ c_{12}^i & c_{22}^i & c_{23}^i & 0 & 0 & 0 \\ c_{13}^i & c_{23}^i & c_{33}^i & 0 & 0 & 0 \\ 0 & 0 & 0 & c_{44}^i & 0 & 0 \\ 0 & 0 & 0 & 0 & c_{55}^i & 0 \\ 0 & 0 & 0 & 0 & 0 & c_{66}^i \end{bmatrix} \begin{bmatrix} \epsilon_{rr}^{(i)} \\ \epsilon_{\theta\theta}^{(i)} \\ \epsilon_{zz}^{(i)} \\ \gamma_{\theta z}^{(i)} \\ \gamma_{rz}^{(i)} \\ \gamma_{r\theta} \end{bmatrix}, \quad i=f_1,c,f_2 \tag{10d}$$

the buckling Eqs. (1) result in the following two linear homogeneous ordinary differential equations of the second order for $U_i(r)$, $V_i(r)$, where $i=f_1$ for $R_1\leq r\leq R_1+f_1$; $i=c$ for $R_1+f_1\leq r\leq R_2-f_2$ and $i=f_2$ for $R_2-f_2\leq r\leq R_2$.

$$c_{11}^{(i)} U_i'' + \frac{c_{11}^{(i)}}{r} U_i' - \left[\left(c_{66}^{(i)} + \frac{\sigma_{\theta\theta}^{0(i)}}{2} \right) n^2 + c_{22}^{(i)} \right] \frac{U_i}{r^2} + \left(c_{12}^{(i)} + c_{66}^{(i)} - \frac{\sigma_{\theta\theta}^{0(i)}}{2} \right) \frac{n V_i'}{r} - \left(c_{22}^{(i)} + c_{66}^{(i)} + \frac{\sigma_{\theta\theta}^{0(i)}}{2} \right) \frac{n V_i}{r^2} = 0 \tag{11a}$$

and

Table 1 Material properties; 1≡r, 2≡θ, 3≡z

Material	E_2 GPa	$E_1=E_3$ GPa	G_{31} GPa	$G_{12}=G_{23}$ GPa	ν_{31}	$\nu_{21}=\nu_{23}$
FACE SHEETS						
Boron/epoxy	221.0	20.7	3.29	5.79	0.45	0.23
Graphite/epoxy	181.0	10.3	5.96	7.17	0.49	0.28
Kevlar/epoxy	75.9	5.52	1.89	2.28	0.47	0.34
CORE						
Alloy foam (isotropic)	0.0459	0.0459	0.0173	0.0173	0.33	0.33

$$\left(c_{66}^{(i)}+\frac{\sigma_{rr}^{0(i)}}{2}\right)V_i''+\left(c_{66}^{(i)}+\sigma_{rr}^{0(i)}-\frac{\sigma_{\theta\theta}^{0(i)}}{2}+\frac{r\sigma_{rr}^{0(i)\prime}}{2}\right)\frac{V_i'}{r}+\left[-\left(c_{66}^{(i)}+c_{22}^{(i)}n^2+\frac{\sigma_{\theta\theta}^{0(i)}}{2}\right)+\frac{r\sigma_{rr}^{0(i)\prime}}{2}\right]\frac{V_i}{r^2}-\left(c_{12}^{(i)}+c_{66}^{(i)}-\frac{\sigma_{rr}^{0(i)}}{2}\right)\frac{nU_i'}{r}+\left[-\left(c_{66}^{(i)}+c_{22}^{(i)}+\frac{\sigma_{\theta\theta}^{0(i)}}{2}\right)+\frac{r\sigma_{rr}^{0(i)\prime}}{2}\right]\frac{nU_i}{r^2}=0. \tag{11b}$$

The associated boundary conditions are as follows:

(a) At the inner and outer bounding surfaces, we have the following two traction conditions at each of the surfaces:

$$c_{11}^{(j)}U_j'+\frac{c_{12}^{(j)}}{r}(U_j+nV_j)=0 \tag{12a}$$

and

$$\left(c_{66}^{(j)}+\frac{\sigma_{rr}^{0(j)}+p_j}{2}\right)V_j'-\left(c_{66}^{(j)}-\frac{\sigma_{rr}^{0(j)}+p_j}{2}\right)\frac{V_j+nU_j}{r}=0, \tag{12b}$$

where $j=f_1$ and $p_j=0$ at $r=R_1$ (inner bounding surface) and $j=f_2$ and $p_j=p$ at $r=R_2$ (outer bounding surface).

(b) At the face-sheet/core interfaces, we have the following four conditions at each of the interfaces:

Traction Continuity:

$$c_{11}^{(j)}U_j'+\frac{c_{12}^{(j)}}{r}(U_j+nV_j)=c_{11}^{(c)}U_c'+\frac{c_{12}^{(c)}}{r}(U_c+nV_c) \tag{13a}$$

and

$$\left(c_{66}^{(j)}+\frac{\sigma_{rr}^{0(j)}}{2}\right)V_j'-\left(c_{66}^{(j)}-\frac{\sigma_{rr}^{0(j)}}{2}\right)\frac{V_j+nU_j}{r}=\left(c_{66}^{(c)}+\frac{\sigma_{rr}^{0(c)}}{2}\right)V_c'-\left(c_{66}^{(c)}-\frac{\sigma_{rr}^{0(c)}}{2}\right)\frac{V_c+nU_c}{r}. \tag{13b}$$

Displacement Continuity:

$$U_j=U_c;\quad V_j=V_c, \tag{13c}$$

where $j=f_1$ at $r=R_1+f_1$ (inner face-sheet/core interface) and $j=f_2$ at $r=R_2-f_2$ (outer face-sheet/core interface).

Solution of the Eigen-Boundary-Value Problem for Differential Equations. Equations (11)–(13) constitute an eigenvalue problem for differential equations, with p the parameter (two point boundary value problem). An important point is that $\sigma_{rr}^{0(i)}(r)$, $\sigma_{\theta\theta}^{0(i)}(r)$ and $\sigma_{rr}^{0(i)'}(r)$ depend *linearly* on the external pressure, p (the parameter) through expressions in the form of Eqs. (8) and this makes possible the direct application of standard solution techniques.

With respect to the method used there is a difference between the present problem and the one for the homogeneous orthotropic body solved by Kardomateas [3]. The complication in the present problem is due to the fact that the displacement field is continuous but has a slope discontinuity at the face-sheet/core interfaces. This is the reason that the displacement field was not defined as one

Table 2 Critical pressure in N/m². Geometry: *f*=0.1 in., *c*=1.0 in. and *B*=3 in.

R_0/h	Elasticity	Classical shell[a] no shear (% versus elast)	Shell w/shear[b] based on core only (% versus elast)	Shell w/shear[c] based on $\bar{G}$ (% versus elast)
BORON/EPOXY faces w/ALLOY-FOAM core				
15	741,773	6,898,740 (+930.0%)	651,125 (−12.2%)	899,768 (+21.3%)
30	277,305	862,343 (+310.9%)	253,721 (−8.5%)	323,361 (+16.6%)
60	70,416	107,793 (+53.0%)	67,383 (−4.3%)	76,087 (+8.0%)
120	11,817	13,474 (+14.0%)	11,717 (−0.85%)	12,203 (+3.3%)
GRAPHITE/EPOXY faces w/ALLOY-FOAM core				
15	720,842	5,650,460 (+783.9%)	637,826 (−11.5%)	874,654 (+21.3%)
30	258,549	706,307 (+273.2%)	238,236 (−7.9%)	298,643 (+15.5%)
60	61,528	88,288 (+43.5%)	59,207 (−3.8%)	65,825 (+7.0%)
120	9,918	11,036 (+11.3%)	9,829 (−0.9%)	10,168 (+2.5%)
KEVLAR/EPOXY faces w/ALLOY-FOAM core				
15	605,472	2,370,590 (+391.5%)	551,668 (−8.9%)	719,856 (+18.9%)
30	171,351	296,324 (+72.9%)	162,433 (−5.2%)	188,347 (+9.9%)
60	31,418	37,040 (+17.9%)	30,712 (−2.2%)	32,397 (+3.1%)
120	4,476	4,630 (+3.4%)	4,403 (−1.6%)	4,470 (−0.13%)

[a]Equation (14).
[b]Equation (17).
[c]Equation (18*b*).

Table 3 Critical pressure in N/m^2. Effect of increased face thickness: f=0.3 in., c=0.6 in., and B=3 in.

R_0/h	Elasticity	Classical shell no shear (% versus elast)	Shell w/shear based on core only (% versus elast)	Shell w/shear based on $\bar{G}$ (% versus elast)
GRAPHITE/EPOXY faces w/ALLOY-FOAM core				
15	1,244,010	11,731,900 (+943.1%)	416,091 (−66.6%)	1,501,160 (+20.7%)
30	393,573	1,466,490 (+372.6%)	188,038 (−52.2%)	542,378 (+37.8%)
60	105,699	183,311 (+73.4%)	67,900 (−35.8%)	128,553 (+21.6%)
120	19,297	22,914 (+18.7%)	16,081 (−16.7%)	20,709 (+7.3%)

function but as three distinct functions for $i=f_1$, c, and f_2, i.e., the two face sheets and the core. Our formulation of the problem employs, hence, "internal" boundary conditions at the face-sheet/core interfaces, as outlined above. Due to this complication, the shooting method [15] was deemed to be the best way to solve this eigen-boundary-value problem for differential equations. A special version of the shooting method was formulated and programmed for this problem. In fact, for each of the three constituent phases of the sandwich structure, we have five variables: $y_1=U_i$, $y_2=U_i'$, $y_3=V_i$, $y_4=V_i'$, and $y_5=p$. The five differential equations are: $y_1'=y_2$, the first equilibrium Eq. (11a), $y_3'=y_4$, the second equilibrium Eq. (11b) and $y_5'=0$.

The method starts from the inner boundary $r=R_1$ and integrates the five first order differential equations from R_1 to the inner face-sheet/core interface R_1+f_1 (i.e., through the inner face sheet). At the inner bounding surface, R_1, we have three conditions, the two traction boundary conditions, Eqs. (12), and a third condition of (abritrarily) setting $U_{f1}=1.0$, therefore we have two freely specifiable variables. The freely specifiable starting values at R_1 are taken as the y_5 (pressure), and the y_3 (V_{f1}) and these are taken as the values from the shell theory (described later). Then, the three boundary conditions at r_1 allow finding the starting values for y_1, y_2 and y_4. Once we reach the inner face-sheet/core interface, R_1+f_1, the tractions from the inner face-sheet side are calculated; these should equal the tractions from the core side, according to the boundary conditions on the face-sheet/core interface, Eqs. (13a) and (13b). This allows finding the slopes of the displacements, $y_2=U_c'$ and $y_4=V_c'$, for starting the shooting into the core (notice that the other three functions, $y_1=U_c$, $y_3=V_c$, and $y_5=p$ are continuous according to Eq. (13c), and their values at R_1+f_1 have already been found at the end of the integration step through the inner face sheet). The next step is integrating the five differential equations from R_1+f_1 to R_2-f_2, i.e., through the core. In a similar manner, once we reach the outer face-sheet/core interface, R_2-f_2, the tractions from the core side are calculated; these should equal the tractions from the outer face-sheet side, per Eq. (13a) and (13b), and this allows finding the slopes of the displacements, $y_2=U_{f2}'$ and $y_4=V_{f2}'$, for starting the shooting into the outer-face sheet (again, the other three functions are continuous and their values at R_2-f_2 have already been found at the end of the integration step through the core). The third step is the integration through the outer-face sheet. Once the outer bounding surface, R_2, is reached, the traction boundary conditions, Eqs. (12), which ought to be zero, are calculated. Multi-dimensional Newton–Raphson is then used to develop a linear matrix equation for the two increments to the adjustable parameters, y_5 and y_3, at R_1. These increments are solved for and added and the shooting repeats until convergence. For the integration phase, we used a Runge–Kutta driver with adaptive step size control. The method produced results very fast and without any numerical complication.

Results, Comparison with Shell Theory and Discussion

As an illustrative example, consider a sandwich ring with the following geometry: core, c=25.4 mm (1 in.), face sheets $f_1=f_2=f$=2.54 mm (0.1 in.) and width B=76.2 mm (3 in.). This value for B was chosen in order to assume that buckling is in the plane of the ring and not out of the plane. Note that the sandwich is symmetric about its midsurface. The total thickness of the ring is, thus, $h=2f+c$=30.48 mm (1.2 in.), and is kept constant. The mean radius, R_0, is chosen in such a manner that the ratio R_0/h ranges from 15 to 120.

Material properties for the face sheets and the core are given in Table 1. The core is isotropic alloy foam and the face sheets are boron/epoxy or graphite/epoxy or kevlar epoxy unidirectional with 0 deg. orientation with respect to the hoop direction. Note again that 1 is the radial (r), 2 is the circumferential (θ), and 3 the axial (z) direction.

Notice also that by referring to Eq. (1), the compliance constants for each orthotropic phase are

$$a_{11}=\frac{1}{E_1};\quad a_{22}=\frac{1}{E_2};\quad a_{33}=\frac{1}{E_3};\quad a_{44}=\frac{1}{G_{23}};\quad a_{55}=\frac{1}{G_{31}};$$

$$a_{66}=\frac{1}{G_{12}},$$

$$a_{12}=-\frac{\nu_{21}}{E_2};\quad a_{13}=-\frac{\nu_{31}}{E_3};\quad a_{23}=-\frac{\nu_{32}}{E_3}.$$

Since the shell is considered to be very long, the buckling analysis reduces to that for a ring [12]. If the transverse shear effect is neglected, the expression for the pressure becomes (classical)

Table 4 Critical pressure in N/m^2. Comparison with homogeneous: f=0.1 in., c=1.0 in., and B=3 in.

R_0/h	Elasticity	Clasical shell no shear (% versus elast)	Shell w/shear based on core only (% versus elast)	Shell w/shear based on $\bar{G}$ (% versus elast)
GRAPHITE/EPOXY homogeneous (no sandwich)				
15	12,594,400	13,407,400 (+6.5%)	12,831,500 (+1.9%)	12,924,100 (+2.6%)
30	1,641,360	1,675,930 (+2.1%)	1,657,330 (+0.97%)	1,660,400 (+1.2%)
60	208,228	209,491 (+0.61%)	208,905 (+0.33%)	209,002 (+0.37%)
120	26,180	26,186 (+0.03%)	26,168 (−0.05%)	26,171 (−0.03%)

$$p_{c\ell} = 3\frac{(EI)_{eq}}{BR_0^3}, \tag{14}$$

where $(EI)_{eq}$ is the equivalent bending rigidity, given in terms of the extensional moduli of the face sheets E_f and the core E_c by [16]

$$(EI)_{eq} = w\left[E_f\frac{f^3}{6} + 2E_f f\left(\frac{f}{2}+\frac{c}{2}\right)^2 + E_c\frac{c^3}{12}\right]. \tag{15a}$$

If the transverse shear effect is accounted for, then

$$p_{w/shear} = 3\frac{(EI)_{eq}}{BR_0^3(1+4k_s)}; \quad k_s = \frac{(EI)_{eq}}{CR_0^2}, \tag{16a}$$

where

$$C = \int_A KGdA, \tag{16b}$$

K being a shear correction factor taken as equal to one and G is the transverse shear stiffness of the sandwich cross section.

Two different expressions for C are employed herein. In the first case, it is assumed that only the core contributes, in which case, $C=BcG_{12}^c$ and

$$k_{s1} = \frac{(EI)_{eq}}{BcG_{12}^cR_0^2}, \tag{17}$$

where G_c is the shear modulus of the core.

In the second case, an effective shear modulus for the sandwich section, $\bar{G}$, which includes the contribution of the facings, is derived based on the compliances of the constituent phases [16]. The expression for $\bar{G}$ is given by

$$\frac{2f+c}{\bar{G}} = \frac{2f}{G_{12}^f} + \frac{c}{G_{12}^c}, \tag{18a}$$

where G_{12}^f is the shear modulus of the facings. Therefore, in this case

$$k_{s2} = \frac{(EI)_{eq}}{B(2f+c)\bar{G}R_0^2}. \tag{18b}$$

Table 2 gives the critical pressure from the elasticity formulation for a range of mean radius over total thickness ratios, in comparison with the classical shell and the two shear deformable shell formulas.

In all cases, $n=2$ was used in the buckling modes, Eq. (9). This has been well established for isotropic cylindrical shells under external pressure; however, since we are dealing with a sandwich structure whose core has elastic properties that are orders of magnitude different from those of the face sheets, verification of this postulate was needed. Indeed, in all cases examined, an exhaustive search was made for the n that results in the minimum eigenvalue, and it was indeed found that $n=2$ corresponds to the lowest eigenvalue. For example, for the case of graphite/epoxy faces with alloy-foam core and $R_0/h=30$, the eigenvalues found from the elasticity solution were (in N/m^2) as follows: $(n=2;258,549)$, $(n=3;397,355)$, $(n=4;469,798)$, $(n=5;512,410)$.

Now coming to the results in Table 2, it is seen that the classical (no shear) formula can yield results highly nonconservative, even approaching ten times the elasticity value for the lower ratio of R_0/h and boron/epoxy case. Both shear correction formulas yield reasonable results with the shear correction formula based on the core only being in general conservative as opposed to the shear correction formula based on an "effective shear modulus," $\bar{G}$, which is nonconservative.

An illustration of the results in Table 2 is provided in Fig. 2, which shows the critical pressure, p_{cr}, normalized with the simple formula from classical shell theory, $p_{c\ell}$, Eq. (14), as a function of the mean radius over thickness ratio, R_0/h. The results are derived from the elasticity formulation and the two shell theory formulas with transverse shear, for the case of graphite/epoxy faces with alloy-foam core. The results show clearly the very significant effect of transverse shear as the ratio R_0/h becomes smaller (thicker shell), in the sense that p_{cr} is only about 12% of the $p_{c\ell}$ (which ignores transverse shear) for $R_0/h=15$. It is also seen that the elasticity results are between the two shells with shear correction formulas, as already discussed in the previous paragraph. For thinner shells, the transverse shear effects get diminished; for example, for $R_0/h=120$, the p_{cr} is about 90% of the $p_{c\ell}$.

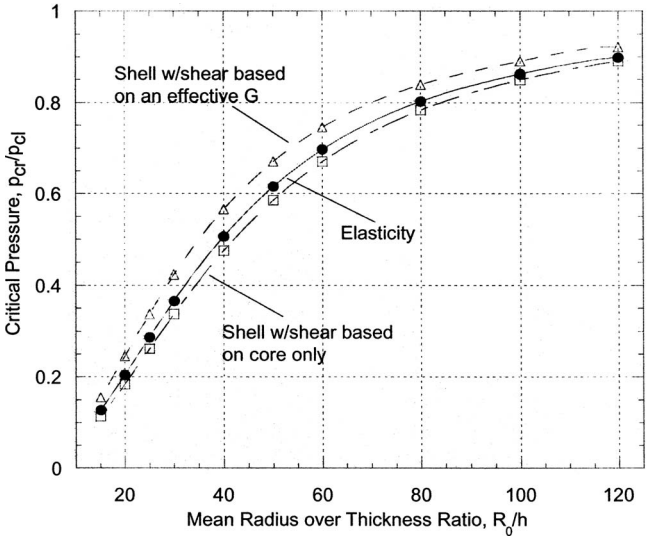

Fig. 2 Critical pressure, p_{cr}, normalized with the classical shell formula, $p_{c\ell}$, Eq. (14)

In the results presented in Table 2, the face sheets were quite thin and the shear correction formula based on the core only, Eq. (17), seemed to be more accurate. In order to further examine this premise, the critical load was calculated for a construction in which the total thickness remains the same but the face sheet thickness is increased at the expense of the core. The results, listed in Table 3, show that the shear correction formula based on an effective modulus (which includes the core), Eq. (18*b*), is now more accurate.

In order to compare with the homogeneous, monolithic, Table 4 gives the critical pressure for a construction made of graphite/epoxy homogeneous, i.e., no sandwich. It is seen that the differences from the elasticity values are modest, even with the classical shell formula. This illustrates the nature of sandwich construction, in which buckling is a more demanding issue.

Acknowledgment

The financial support of the Office of Naval Research, Ship Structures and Systems, S & T Division, Grant Nos. N00014-90-J-1995 and N00014-0010323, and the interest and encouragement of the Grant Monitor, Dr. Y. D. S. Rajapakse, are both gratefully acknowledged.

References

[1] Hutchinson, J. W., 1968, "Buckling and Initial Postbuckling Behavior of Oval Cylindrical Shells Under Axial Compression," J. Appl. Mech., **35**, pp. 66–72.
[2] Budiansky, B., and Amazigo, J. C., 1968, "Initial Post-Buckling Behavior of Cylindrical Shells Under External Pressure," J. Math. Phys. (Cambridge, Mass.), **47**(3), pp. 223–235.
[3] Kardomateas, G. A., 1993a, "Buckling of Thick Orthotropic Cylindrical Shells Under External Pressure," ASME J. Appl. Mech., **60**, pp. 195–202.
[4] Kardomateas, G. A., and Chung, C. B., 1994, "Buckling of Thick Orthotropic Cylindrical Shells Under External Pressure Based on Non-Planar Equilibrium Modes," Int. J. Solids Struct., **31**(16), pp. 2195–2210.
[5] Kardomateas, G. A., 1993b, "Stability Loss in Thick Transversely Isotropic

Cylindrical Shells Under Axial Compression," ASME J. Appl. Mech., **60**, pp. 506–513.
[6] Kardomateas, G. A., 1995, "Bifurcation of Equilibrium in Thick Orthotropic Cylindrical Shells Under Axial Compression," ASME J. Appl. Mech., **62**, pp. 43–52.
[7] Soldatos, K. P., and Ye, J.-Q., 1994, "Three-Dimensional Static, Dynamic, Thermoelastic, and Buckling Analysis of Homogeneous and Laminated Composite Cylinders," Compos. Struct., **29**, pp. 131–143.
[8] Lekhnitskii, S. G., 1963, *Theory of Elasticity of an Anisotropic Elastic Body*, Holden Day, San Francisco, also Mir, Moscow, 1981.
[9] Kardomateas, G. A., 2001, "Elasticity Solutions for a Sandwich Orthotropic Cylindrical Shell Under External Pressure, Internal Pressure and Axial Force," AIAA J., **39**(4), pp. 713–719.
[10] Birman, V., and Simitses, G. J., 2000, "Theory of Cylindrical Sandwich Shells with Dissimilar Facings Subjected to Thermo-mechanical Loads," AIAA J., **37**(12), pp. 362–367.
[11] Birman, V., Simitses, G. J., and Shen, L., 2000, "Stability of Short Sandwich Cylindrical Shells with Rib-Reinforced Facings," *Recent Advances in Applied Mechanics*, J. T. Katsikadelis, D. E. Beskos, and E. E. Gdoutos, eds., National Technical University of Athens, Greece, pp. 11–21.
[12] Birman, V., and Simitses, G. J., 1999, "Stability of Long Cylindrical Sandwich Shells with Dissimilar Facings Subjected to Lateral Pressure," *Advances in Aerospace Materials and Structures*, G. Newaz, ed., ASME AD-58, ASME, New York, pp. 41–51.
[13] Smith, C. V., Jr., and Simitses, G. J., 1969, "Effect of Shear and Load Behavior on Ring Stability," ASCE, J. of EM Division, **95**(3), pp. 559–569.
[14] Simitses, G. J., and Aswani, M., 1974, "Buckling of Thin Cylinders Under Uniform Lateral Loading," ASME J. Appl. Mech., **41**(3), pp. 827–829.
[15] Press, W. H., Flannery, B. P., Teukolsky, S. A., and Vetterling, W. T., 1989, *Numerical Recipes*, Cambridge University Press, Cambridge, UK.
[16] Huang, H., and Kardomateas, G. A., 2002, "Buckling and Initial Postbuckling Behavior of Sandwich Beams Including Transverse Shear," AIAA J., **40**(11), pp. 2331–2335.